Single-Carrier Space-Time Trellis and Space-Time Block Coding for Dispersive Rayleigh Fading Channels

S. X. Ng, T. H. Liew, B. L. Yeap, E. L. Kuan and [1]L. Hanzo

Dept. of ECS, University of Southampton, SO17 1BJ, UK.
Tel: +44-23-8059 3125, Fax: +44-23-8059 4508
Email: [1]lh@ecs.soton.ac.uk, http://www-mobile.ecs.soton.ac.uk

Abstract – **In this contribution we propose a novel Space-Time Coding (STC) scheme for transmissions over dispersive Rayleigh fading channels, which invokes a Joint-Detection assisted Minimum Mean Square Error based Decision Feedback Equalizer (JD-MMSE-DFE) for jointly detecting the channel-impaired wideband signals of multiple transmit antennas. The performance of the proposed scheme was investigated using Quadrature-Phase-Shift-Keying (QPSK) when communicating over channels exhibiting multi-path components. It was shown that the scheme advocated outperforms conventional STC due to benefitting from the multi-path diversity of the dispersive channel.**

1. INTRODUCTION

In numerous practical situations the wireless channels are neither highly time selective nor significantly frequency selective. This motivated numerous researchers to investigate space diversity techniques with the aim of improving the system's performance. On one hand, receiver diversity [1] has been widely used at the base stations of both the GSM and IS-136 systems. On the other hand, recently the family of transmit diversity techniques [2] has been studied extensively for employment at the base station, since it is more practical to have multiple transmit antennas at the base station, than at the mobile handset. Space-Time Trellis Coding (STTC) pioneered by Tarokh *et al.* [3] combines signal processing at the receiver with intelligent coding techniques appropriately mapping the information to be transmitted to multiple transmit antennas. In an attempt to reduce the associated decoding complexity, Alamouti proposed Space-Time Block Coding [4] (STBC) employing two transmit antennas. Alamouti's scheme was later generalized to an arbitrary number of transmit antennas [5].

Space-Time Coding (STC) schemes were originally proposed for transmission over narrowband fading channels. When encountering wideband channels, multi-carrier Code Division Multiple Access (MC-CDMA) and Orthogonal Frequency Division Multiplexing (OFDM) [6] can be utilised for converting the wideband channel to numerous narrowband channels. These transmission schemes can then be concatenated with conventional narrowband STC schemes [7, 8]. The resultant concatenated schemes provide significant coding gain and diversity gain over uncoded single-transmitter and single-receiver schemes, typically at the expense of utilising an increased bandwidth, which is required for accommodating multiple replicas of the transmitted signal using multiple carriers. In single carrier systems STC can also be advantageously combined with Multiple-Input-Multiple-Output (MIMO) equalizers [9] as well as with turbo equalization schemes [10] for mitigating the Inter Symbol Interference (ISI) induced by the multi-path channel. In [9] STBC is combined with the MIMO equalizer of [11], where the number of receivers is at least the same as the number of transmitters.

In our proposed system the Minimum Mean Square Error Decision Feedback Equalizer (MMSE-DFE) based Joint Detection (JD) scheme [12] is used, which constitutes a widely known powerful approach for mitigating the effects of both multi-user interference and ISI. However, in this particular application the JD scheme will not be employed for detecting multiple users, it rather will be used for mitigating the effects of employing multiple transmitters and the channel-induced ISI. Since the JD is capable of jointly detecting all the transmitted signals arriving from the multiple transmit antennas, we argue that it can be concatenated with STC for detecting the ISI-contaminated signals arriving from the multiple transmitters, which may also interfer with each other.

The rest of this treatise is organised as follows. Our system overview is presented in Section 2, the JD-MMSE-DFE is discussed in Section 2.1, while STTC and STBC are briefly highlighted in Section 2.2. Our simulation results are discussed in Section 3 and finally our conclusions are offered in Section 4.

2. SYSTEM OVERVIEW

The block diagram of the Joint Detection assisted Minimum Mean Square Error based Decision Feedback Equalised Space-Time Coding (STC-JD-DFE) system is shown in Figure 1. We consider QPSK based 8-state STTC [3] as well as QPSK aided STBC using Alamouti's G_2 code [4], where two transmit antennas are utilised. We apply two different spreading codes to the two transmit antennas before transmission. Hence the information symbol s is encoded by the Space-Time Trellis (STT) encoder into the symbols d_1 and d_2, which are spread before transmission by the spreading codes c^1 and c^2, respectively. The received signal y is the superposition of the two transmitted signals as well as the multi-path components of the signals. At the JD-MMSE-DFE assisted receiver, joint detection is performed, in order to jointly detect the two transmitted signals, yielding $\hat{d}_1$ and $\hat{d}_2$. Finally, the detected signals are passed to the ST decoder for generating an estimate of the information symbol $\hat{s}$. Again, this scheme can be viewed as being equivalent to a two-user scenario in the context of a single-transmitter JD-MMSE-DFE CDMA system. However, for a K transmit antenna aided STC scheme each transmitter transmits

0-7803-7467-3/02/$17.00 ©2002 IEEE.

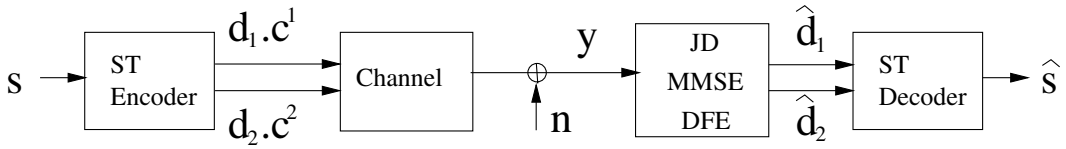

Figure 1: Block diagram of the concatenated STC and JD-MMSE-DFE scheme.

only a fraction $1/K$ of the total transmit energy.

2.1. The JD-MMSE-DFE Subsystem

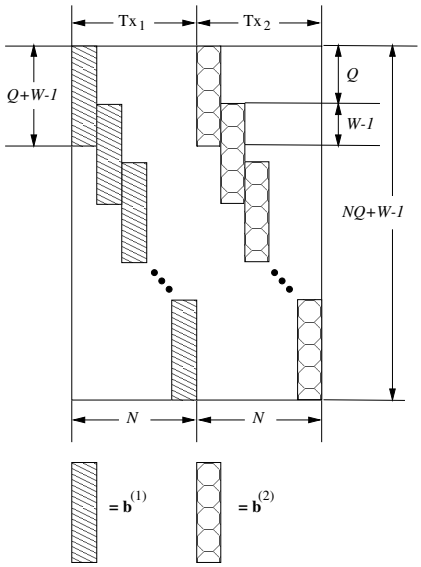

Figure 2: Example of the system matrix $\mathbf{A}$ for a two-transmitter system, where $\mathbf{b}^{(1)}$ and $\mathbf{b}^{(2)}$ are column vectors representing the combined impulse responses of transmitter (Tx) 1 and 2, respectively, in Equation 2. The notations are as follows: N denotes the number of data symbols transmitted by each transmitter, Q represents the number of chips in each spreading sequence and W indicates the length of the wideband channel impulse response (CIR).

Let us consider the structure of the system matrix $\mathbf{A}$ for the two-transmitter system of Figure 2. The combined impulse response, $\mathbf{b}_n^{(k)}$, due to the spreading sequence $\mathbf{c}^{(k)}$ and the channel impulse response (CIR) $\mathbf{h}_n^{(k)}$ is defined by the convolution of $\mathbf{c}^{(k)}$ and $\mathbf{h}_n^{(k)}$, which is represented as:

$$\begin{aligned} \mathbf{b}_n^{(k)} &= (b_n^{(k)}(1), b_n^{(k)}(2), \ldots, \\ &\quad b_n^{(k)}(l), \ldots, b_n^{(k)}(Q+W-1))^T \quad (1) \\ &= \mathbf{c}^{(k)} * \mathbf{h}_n^{(k)}, \quad (2) \\ &\quad \text{for } k = 1 \ldots K; \;\; n = 1, \ldots N, \end{aligned}$$

where K is the total number of transmitters, N denotes the number of data symbols transmitted by each transmitter, Q represents the number of chips in each spreading sequence and W indicates the length of the wideband CIR. The system matrix of the k^{th} transmitter, $\mathbf{A}^{(k)}$ is represented by:

$$[\mathbf{A}^{(k)}]_{in} = \begin{cases} b_n^{(k)}(l) & \text{for } i = (n-1)Q + l; \\ & n = 1, \ldots, N; \\ & l = 1, \ldots, Q+W-1; \\ 0 & \text{otherwise.} \end{cases} \quad (3)$$

The overall system matrix can be constructed by appending the $\mathbf{A}^{(k)}$ matrix of each of the K transmitters column-wise:

$$\mathbf{A} = (\mathbf{A}^{(1)}, \mathbf{A}^{(2)}, \ldots, \mathbf{A}^{(k)}, \ldots, \mathbf{A}^{(K)}). \quad (4)$$

Therefore, the discretised received composite signal can be represented in matrix form as :

$$\begin{aligned} \mathbf{y} &= \mathbf{A}\mathbf{d} + \mathbf{n}, \quad (5) \\ \mathbf{y} &= (y_1, y_2, \ldots, y_{NQ+W-1})^T, \end{aligned}$$

where $\mathbf{n} = (n_1, n_2, \ldots, n_{NQ+W-1})^T$, is the noise sequence, which has a covariance matrix of $\mathbf{R}_n = E[\mathbf{n}.\mathbf{n}^H]$. The composite signal vector $\mathbf{y}$ has $(NQ + W - 1)$ elements for a data burst of length N symbols.

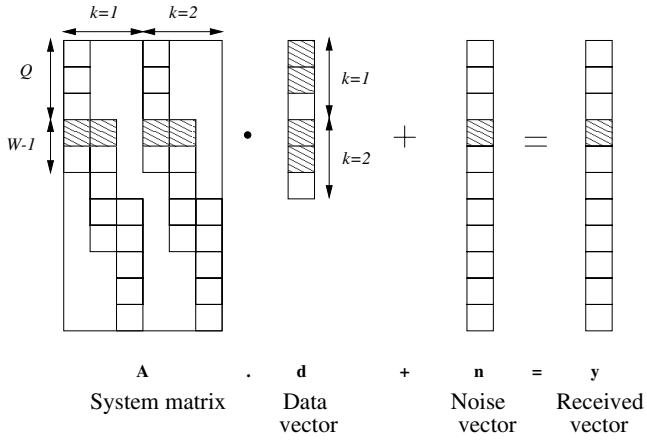

Figure 3: Example of the matrix equation $\mathbf{y} = \mathbf{A}\mathbf{d} + \mathbf{n}$ for a $K = 2$–transmitter system. Each transmitter transmits $N = 3$ symbols per transmission burst and each symbol is spread with the aid of a random spreading sequence of length $Q = 3$ chips. The channel associated with each transmitter has a dispersion of $W = 3$ chip durations. The shaded boxes indicate the data positions of the matrices involved in computing the fourth element of the received signal vector, $\mathbf{y}$.

Figure 3 shows the stylized structure of Equation 5 for a specific example. In the figure, a system having $K = 2$ transmitters is depicted. Each transmitter transmits $N = 3$ symbols per transmission burst and each symbol is spread with the aid of a signature sequence of length $Q = 3$ chips. The channel associated with each transmitter has a dispersion of $W = 3$ chip durations. The basic concept of joint

detection is centred around processing the received composite signal vector, $\mathbf{y}$, in order to determine the transmitted data vector, $\mathbf{d}$. The operations required for obtaining the JD-MMSE-DFE data estimates can be summarised as follows. First we construct the system matrix $\mathbf{A}$ of Equation 4. Then we obtain the output of the Whitening Matched Filter (WMF) as follows [13]:

$$\hat{\mathbf{d}}_{\mathbf{WMF}} = \mathbf{A}^H \mathbf{R}_n^{-1} \mathbf{y}, \quad (6)$$

where $\mathbf{A}^H$ is the conjugate transpose of $\mathbf{A}$ and $\mathbf{R}_n^{-1}$ is the inverse of the noise covariance matrix $\mathbf{R}_n$. Next, Cholesky decomposition [14] of the matrix $(\mathbf{A}^H \mathbf{R}_n^{-1} \mathbf{A} + \mathbf{R}_d^{-1})$ is performed, yielding:

$$\mathbf{A}^H \mathbf{R}_n^{-1} \mathbf{A} + \mathbf{R}_d^{-1} = (\mathbf{DU})^H \mathbf{DU}, \quad (7)$$

where $\mathbf{R}_d^{-1}$ is the inverse of the signal's covariance matrix $\mathbf{R}_d$, $\mathbf{D}$ is a diagonal matrix having real-valued elements and $\mathbf{U}$ is an upper triangular matrix, where all the elements on its main diagonal have the value of one. Consequently, the JD-MMSE-DFE scheme's feed-forward filter output is obtained by solving the equation [12]:

$$\begin{aligned} \hat{\mathbf{y}} &= (\mathbf{D})^{-1} ((\mathbf{DU})^H)^{-1} \mathbf{A}^H \mathbf{R}_n^{-1} \mathbf{y} \\ &= (\mathbf{D})^{-1} ((\mathbf{DU})^H)^{-1} \hat{\mathbf{d}}_{\mathbf{WMF}}. \end{aligned} \quad (8)$$

Finally the feedback operation is invoked for producing the final data estimate as follows [12]:

$$\hat{d}_i(\text{MMSE-BDFE}) = \hat{y}_i - \sum_{j=i+1}^{J=KN} [\mathbf{U}]_{ij} \hat{t}_j, \quad (9)$$

where $\hat{t}_j$ is the hard decision based value of the feedback estimate $\hat{d}_j$.

2.2. The STC Subsystem

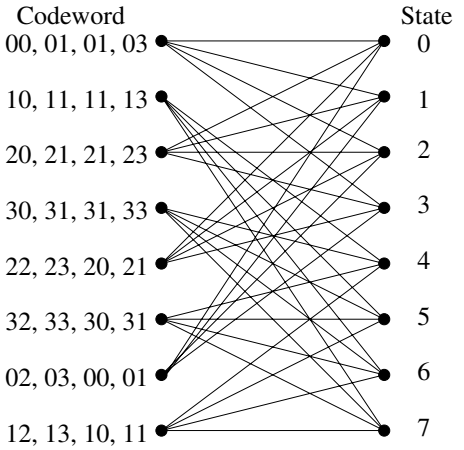

Figure 4: Trellis diagram of the 8-state STTC using two transmitters and QPSK modulation [5].

Space-Time Trellis Coding: Figure 4 shows the trellis diagram of the conventional 8-state STTC scheme utilising two transmit antennas and QPSK modulation. At the left of the trellis diagram we see the STTC codewords $\{d_1, d_2\}$. As seen in Figure 4, there are four branches emerging from each trellis state, since there are four possible QPSK symbols, namely $\{0, 1, 2, 3\}$. The STT encoder maps each of the quaternary QPSK information symbols to two QPSK symbols constituting a STTC codeword as seen at the left of Figure 4 and changes its state according to the trellis. Finally, the STTC symbols are transmited simultaneously using two transmit antennas. In the conventional narrowband STTC scheme designed for transmission over single-path fading channels utilising two transmit and one receive antennas, the branch metric associated with a trellis transition is given by [3]:

$$\left| y - (h_1 d_1 + h_2 d_2) \right|^2, \quad (10)$$

where h_i is the CIR experienced by the signal emitted from transmitter i, while d_1 and d_2 are the legitimate QPSK symbols. In a single-path scenario Equation 10 effectively represents a form of channel equalization, where the non-dispersive sungle-tap CIR is multiplied by the legitimate QPSK symbols, when computing the branch metric. However, this simple single-tap equalization scheme cannot be used in multi-path channels, where convolutional-based multi-tap equalization has to be applied to the received signal y, in order to yield its best approximation $\hat{y}$. In the context of STTC using two transmitters, this approximation is given by:

$$\hat{y} = \hat{d}_1 + \hat{d}_2, \quad (11)$$

which is the sum of the outputs generated by the JD-MMSE-DFE of Figure 1. Then the branch metric associated with a trellis transition of the STTC scheme is given by:

$$\left| \hat{y} - (d_1 + d_2) \right|^2 = \left| (\hat{d}_1 - d_1) + (\hat{d}_2 - d_2) \right|^2. \quad (12)$$

The Viterbi algorithm is then used for finding the trellis path having the lowest accumulated metric.

Table 1: The G_2 STBC encoding procedure portrayed over the time slots t_1 and t_2, utilising the transmit antennas Tx_1 and Tx_2 for transmitting the information symbols S_1 and S_2, where $*$ denotes complex conjugate.

	t_1	t_2
Tx_1	S_1	$-S_2^*$
Tx_2	S_2	S_1^*

Space-Time Block Coding: As for STBC using Alamouti's G_2 code [4, 5], the encoding scheme requires two time slots and two transmit antennas for transmitting two information symbols, namely S_1 and S_2. Specifically, the G_2 STBC procedure is shown in Table 1. Over the duration of two time slots the JD-MMSE-DFE receiver generates four outputs, namely $\hat{d}_1$, $\hat{d}_2$, $\hat{d}_3$ and $\hat{d}_4$. However, we know that $\hat{d}_3$ and $\hat{d}_4$ correspond to $-S_2^*$ and S_1^* in Table 1 respectively. Hence the branch metrics related to S_1 and S_2 can be computed from:

$$\left| (\hat{d}_1 + \hat{d}_4^*) - d_1 \right|^2 = \left| (\hat{S}_1^1 + \hat{S}_1^2) - S_1 \right|^2, \quad (13)$$

$$\left| (\hat{d}_2 - \hat{d}_3^*) - d_2 \right|^2 = \left| (\hat{S}_2^1 + \hat{S}_2^2) - S_2 \right|^2, \quad (14)$$

where $\hat{S}^t$ denotes the estimate of S at timeslot t. Finally, hard decisions are carried out using Equation 13 for S_1 and Equation 14 for S_2.

Table 2: Parameters of the STC-JD-DFE system.

Parameter	Value
Number of equal-weight CIR paths	3, 4 and 5
Doppler frequency	80 Hz
Spreading factor, Q	8
Chip rate	2.167 MBaud
Number of QAM symbols per JD block, N	20
Modulation mode	QPSK
Number of STTC states	8
STBC code	G_2 [4, 5]
Number of transmitters	2

3. SIMULATION RESULTS AND DISCUSSIONS

Let us now investigate the performance of the proposed wideband STC-JD-DFE scheme using the simulation parameters shown in Table 2, where 8-chip random spreading codes were utilised for separating the two transmitters of both the 8-state STTC scheme as well as that of the G_2 STBC scheme. QPSK modulation was considered and this gave a throughput of two information bits per symbol. We assumed that the receiver perfectly knows the 3, 4 or 5-path equal-weight CIRs, while the fading is constant for the duration of the JD block of 20 symbols. The channel models used exhibit equal power for each of the multi-path components and each path is faded according to independent Rayleigh fading statistics, as described by the parameters of Table 2.

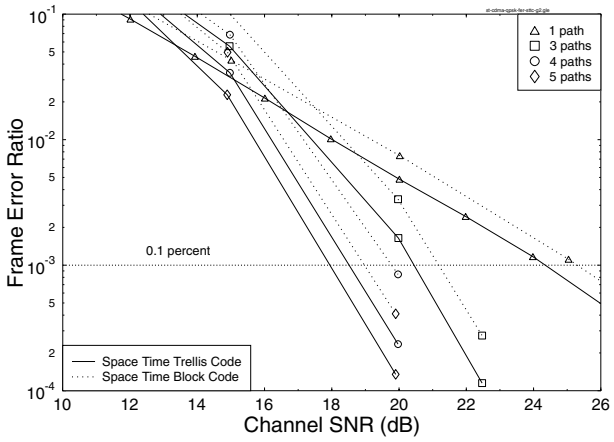

Figure 5: Frame Error Ratio (FER) versus Signal to Noise Ratio (SNR) performance of conventional narrowband STC for transmissions over a single-path Rayleigh fading channel and that of the proposed STC-JD-DFE system for transmissions over Rayleigh fading channels exhibiting 3, 4 and 5 resolvable paths, utilising the simulation parameters of Table 2.

Figure 5 portrays our Frame Error Ratio (FER) performance comparisons between the conventional narrowband STC for transmission over a single-path Rayleigh fading channel and for the STC-JD-DFE scheme utilising the parameters of Table 2 for transmissions over Rayleigh fading channels having 3, 4 and 5 equal-weight paths. The proposed wideband STC-JD-DFE scheme exhibits a significant performance gain over the narrowband STC scheme, since it is capable of exploiting the multi-path diversity with the advent of utilising the JD-MMSE-DFE assisted wideband receiver. To elaborate a little further, the conventional narrowband STC scheme is incapable of adequately operating in wideband propagation conditions due to the inteference of the different antennas' signals. By contrast, the proposed wideband STC-JD-DFE scheme introduced JD and equalization of the signals and hence in fact benefits from the multipath diversity.

Comparing the proposed wideband **JD-MMSE-DFE aided STTC** scheme with the conventional narrowband STTC arrangement, an approximately $3.7\ dB$ gain is obtained by the proposed scheme at FER = 10^{-3} for transmission over a three-path channel in comparisons to the conventional narrowband STTC scheme communicating over a single-path channel. Another $2\ dB$ SNR improvement is obtained, when the channel exhibits four resolvable paths. However, less than $1\ dB$ further improvement is obtained, when the channel has five resolvable paths. Similar performance trends can be observed, when comparing the proposed **JD-MMSE-DFE aided STBC** scheme with the conventional narrowband STBC arrangement. An approximately $4\ dB$ gain is obtained by the proposed wideband scheme at FER=10^{-3}, when communicating over a three-path channel in comparisons to the conventional narrowband STBC scheme transmitting over a single-path channel. Another $1.2\ dB$ further improvement is obtained, when the channel exhibits four paths. However, less than $1\ dB$ further improvement is obtained, when the channel has 5 resolvable paths. Explicitly, the new scheme provides significant performance improvements for transmissions over channels exhibiting a low number of paths, but the additional improvements gradually erode, as the number of paths increases.

Comparing the proposed wideband STTC and STBC schemes, STTC performs better, than STBC in terms of the achievable FER for transmissions over multi-path channels. The SNR gains of STTC over STBC at FER=10^{-3} are: $0.8\ dB$ for three-path, $1.3\ dB$ for four-path and $1.1\ dB$ for five-path channels. In other words, STTC schemes are capable of achieving an approximately $1\ dB$ SNR gain at FER=10^{-3} over the G_2-coded STBC schemes in the context of multi-path channels. This gain is attributable to the fact that STTC invokes an extra Viterbi decoding at the receiver, which improves its performance in comparison to the G_2 STBC scheme, where only simple combining of the received signals is invoked at the receiver. However, when additional channel codecs are concatenated with the STBC scheme, it outperforms the STTC scheme at the same decoding complexity and same throughput [8]. This suggests that when invoking concatenated channel codes and simultaneously expanding the modulation order for maintaining the uncoded throughput, STBCs are more efficient than STTC arrangement.

Let us now investigate the Bit Error Ratio (BER) performance of the scheme. Figure 6 portrays our BER performance comparisons between the conventional STC for transmissions over a single-path Rayleigh fading channel and for the STC-JD-DFE scheme utilising the parameters of Table 2 for transmissions over dispersive Rayleigh fading channels having 3, 4 and 5 paths. Again the proposed STC-JD-DFE scheme exhibits a better performance than the narrowband STC arrangement. Specifically, significant performance improvements were achieved for transmissions over channels exhibiting a low number of paths, but the additional improvements gradually

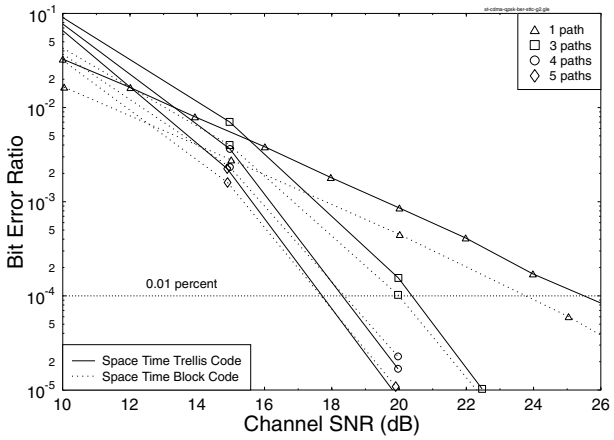

Figure 6: Bit Error Ratio (BER) versus Signal to Noise Ratio (SNR) performance of conventional STC for transmissions over a single-path Rayleigh fading channel and that of the proposed STC-JD-DFE system for transmissions over Rayleigh fading channels exhibiting 3, 4 and 5 resolvable paths, utilising the simulation parameters of Table 2.

eroded, as the number of paths increased. The BER performance of the conventional STBC was found to be better, than that of the conventional STTC for transmissions over narrowband channels, since STTC was originally designed for improving the system's FER. However, the advantage of STBC over STTC decreased, when the channel exhibited a higher number of multi-path components. At a BER=10^{-4}, STTC performed better, than STBC for channels exhibiting four and five resolvable paths.

4. CONCLUSION

In this contribution JD-MMSE-DFE assisted STC was proposed for faciliting wideband STC transmissions over multi-path Rayleigh fading channels. Significant performance gains were observed, when the channel exhibited a low number of resolvable paths, while the additional gains decreased, when the channel exhibited a higher number of paths. The STTC schemes always performed better, than the STBC schemes in terms of their FER for transmissions over both narrowband and wideband channels.

5. ACKNOWLEDGEMENTS

The financial support of the European Union under the auspices of the SCOUT project and the EPSRC, Swindon UK is gratefully acknowledged.

6. REFERENCES

[1] P. Balaban, J. Salz, "Optimum diversity combining and equalization in digital data transmission with application to cellular mobile radio – Part I: Theoretical considerations," *IEEE Transactions on Communications*, vol. 40(5), pp. 885–894, 1992.

[2] A. Wittneben, "Base station modulation diversity for digital SIMULCAST," *IEEE Vehicular Technology Conference*, pp. 505–511, 1993.

[3] V. Tarokh, N. Seshadri and A. R. Calderbank, "Space-time codes for high rate wireless communication: Performance analysis and code construction," *IEEE Transactions on Information Theory*, vol. 44, pp. 744–765, March 1998.

[4] S. M. Alamouti, "A simple transmitter diversity scheme for wireless communications," *IEEE Journal on Selected Areas in Communications*, vol. 16, pp. 1451–1458, October 1998.

[5] V. Tarokh, "Space-Time Block Codes from Orthogonal Designs," *IEEE Transactions on Information Theory*, vol. 45, pp. 1456–1467, July 1999.

[6] L. Hanzo, W. Webb and T.Keller, *Single- and Multi-carrier Quadrature Amplitude Modulation*. New York, USA : John Wiley and Sons, 2000.

[7] B. J. Choi, T. H. Liew and L. Hanzo, "Concatenated Space-Time Block Coded and Turbo Coded Symbol-by-Symbol Adaptive OFDM and Multi-Carrier CDMA Systems," *IEEE Vehicular Technology Conference*, p. 107, May 2001.

[8] T. H. Liew, B. J. Choi and L. Hanzo, "Comparative Study of Concatenated Turbo Coded and Space-Time Block Coded as well as Space-Time Trellis Coded OFDM," *IEEE Vehicular Technology Conference*, p. 107, May 2001.

[9] W. Choi and J. Cioffi, "Space-Time Block Codes over Frequency Selective Rayleigh Fading Channels," *IEEE Vehicular Technology Conference*, pp. 2541–2549, September 1999.

[10] B. L. Yeap, T. H. Liew and L. Hanzo, "Turbo Equalization of Serially Concatenated Systematic Convolutional Codes and Systematic Space Time Trellis Codes," *IEEE Vehicular Technology Conference*, p. 119, May 2001.

[11] A. Duel-Hallen, "Equalizers for multiple input/multiple output channels and PAM systems with cyclostationary input sequences," *IEEE Journal on Selected Areas in Communications*, vol. 10, pp. 630–639, April 1992.

[12] P. Jung and J. Blanz, "Joint detection with coherent receiver antenna diversity in CDMA mobile radio systems," *IEEE Transactions on Vehicular Technology*, vol. 44, pp. 76–88, Feb. 1995.

[13] E. A. Lee and D. G. Messerschmitt, *Digital Communication*. Kluwer Academic Publishers, 1988.

[14] W. H. Press, S. A. Teukolsky, W. T. Vetterling, and B. P. Flannery, *Numerical Recipes in C: The Art of Scientific Computing*. Cambridge University Press, 1993.